# SYNOPSIS


**Name of the Research Scholar:** Shweta Paroha
**Registration no. of Research scholar:** 32/PhD/DPSRU/2018
**Name of Supervisor:** Prof. P. K. Sahoo

**Title of thesis:** "Development and Evaluation of Gemcitabine Nanoparticulate Delivery Strategy for Improved Cancer Chemotherapy"

## 1. Introduction:

Gemcitabine is one of the most potent nucleoside analogue clinically approved for treatment of various solid tumors, including, pancreatic [1], ovarian [2], breast [3] and non-small lung cancers [4]. The clinical applicability of gemcitabine is limited due to rapid enzymatic metabolism and fast kidney excretion. Following intravenous administration gemcitabine get metabolized into its inactive uracil derivative (2, 2 diflurodioxyuridine) by an enzyme, cytidine deaminase (CDA) which is present in plasma [5, 6]. Native gemcitabine internalized into tumor cells, mainly through nucleoside transporters (hENT-1, and hCNT-1) [7]. After entry into the cells, gemcitabine phosphorylated to get convert into its active metabolite, monophosphate and triphosphate by deoxycytidine kinase and pyrimidine nucleotide kinases, respectively [8, 9].

Due to inactivation in systemic circulation gemcitabine showed very short plasma half-life of about (8-17 min after intravenous administration). A high dose (1000-1250 mg/m2) of gemcitabine required to achieve optimum therapeutic concentration. High dose of gemcitabine resulted into some serious toxicities, including, hepatotoxicity, myelosuppression, haematological toxicities and gastrointestinal toxicities and nephrotoxicity [10]. There are several attempts have been made to overcome these limitations, including, nanoparticles [11] polymeric micelles [12] liposomes [13] polymersomes [14] nanovesicles [15] polymer- drug conjugates [16].

In this study, we have conjugated 4-(N) position of gemcitabine with PCL-PEG-PCL co-polymer through amide linkage and disperse into water to form self-assembled nanoparticles. Gemcitabine is hydrophilic drug which needs nucleoside transporter to cross biological barrier and exerts cytotoxicity. We hypothesise that, conjugation with PCL-PEG co-polymer can improve lipophilicity of native drug and facilitate transport across the lipid bilayer, which in turn, could improve its cytotoxic potential. The prepared nanoparticles was characterized by FTIR, NMR, DSC, P-XRD, particle size, polydispersity, zeta potential and morphology. Further, in-vitro analysis, including anti-proliferative activity, ROS, MMP and apoptosis analysis has been performed in various cell lines.

## 2. Hypothesis of the study:

Chemotherapy has several advantages; however, it is associated with a variety of challenges due to lack of selectivity and associated high toxicity. The main reasons for the failure of

chemotherapy is hampered pharmacokinetic profile. Therefore, a harmless, efficient and novel treatment strategy, especially for chemotherapeutic agents are needed to fight against cancer.

Among the chemotherapeutic agents for cancer, nucleoside analogs constitute one of the most important classes of drugs. Gemcitabine is a prototype drug of this class which is active against a wide range of solid tumors. However, short half-life, high dose and dose specific toxicities are major clinical limitation associated of gemcitabine. Since, amino group present in gemcitabine is responsible enzymatic degradation and inactivation of the drug in circulatory system. Thus, we hypothesized that conjugation of 4-(N) position of gemcitabine with PCL-PEG-PCL co-polymer and simultaneous formation of self-assembled nanoparticles can overcome limitation of the drug.

In another study, we prepared Gem loaded BSANPs by desolvation cross-linking method and glutaraldehyde is used as cross linker. The Gem-BSANPs were coated with HA targeted delivery of Gem to CD44 receptor. The NPs were characterized by different parameters, including differential light scattering, morphology by TEM and physical state of the NPs with DSC, in vitro release and hemolysis assay. MTT assay has been used to evaluate in vitro cytotoxicity of free Gem and HA coated Gem NPs on human lung carcinoma (A549) and human breast carcinoma (MCF-7). We hypothesized that HA can specifically target the CD44 receptor overexpressed on different tumor and overcome the limitation of drug.

**3. Objectives:**

The proposed study is designed with the aim to improve therapeutic potential and reduce toxicities associated with gemcitabine. The objectives are as mentioned bellow:

1. Preparation, characterization and evaluation of hyaluronic acid coated bovine serum albumin nanoparticles for anticancer activity.

2. Preparation, characterization and evaluation of Gem conjugated self-assembled nanoparticles for anticancer activity.

**4. Work done during the period:**

**Objective: 1** Preparation, characterization and evaluation of hyaluronic acid coated bovine serum albumin nanoparticles for anticancer activity.

**Preparation of Gem-BSANPs**

Gem encapsulated BSANPs has been prepared by desolvation cross-linking method as reported previously with slight modification [9]. For process optimization, first pH of BSA solution (100 mg/ 2mL) were kept at 6 to 10 and amount of ethanol required for desolvation has been optimized. The particle size, encapsulation efficiency and percent NPs yield were analysed at process. For optimized formulation, 100 mg of BSA and 10 mg of Gem were dissolved in 2 mL of milli-Q water (5% w/v) and the pH of the aqueous solution was maintained at 9 by using of 0.1M NaOH solution. The solution was taken into a 25 mL glass beaker and kept on magnetic stirring at RT. For desolvation, dehydrated ethanol (4-5 mL)

was added into the polymer solution drop-wise by using a 5 mL syringe. The addition of ethanol was done under magnetic stirring of 600 rpm at a rate of 1 mL/min. After formation of NPs, 100 µL of glutaraldehyde (25% solution) was added into the dispersion and the stirring allowed at 400 rpm for further 30 min followed by complete evaporation of ethanol on rotavapor (BUCHI, R-300). The obtained suspension was centrifuged at 18000 rpm for 20 min to obtain the pellet. The pellet was washed with PBS (pH 7.4) to remove unreacted glutaraldehyde and un-encapsulated drug.

**Preparation of HA-Gem-BSANPs**

The HA was coated on the Gem-BSANPs as per the previously reported method with a few modifications [21]. The HA was first activated for surface coupling of Gem-BSANPs. For activation, HA (60 mg) was dissolved in 1 mL of distilled water and then EDC (57.5 mg) and NHS (34.5 mg) were added into the HA solution. The solution was kept on stirring for 1 hour at RT for activation of carboxylic groups of HA. The solution was then dialyzed (MWCO 2 kDa) against distilled water to remove unreacted moiety and lyophilized for 24 hours to obtain solid HA powder. The Gem-BSANPs were reconstituted into distilled water with HA (2 mg/mL). The dispersion was incubated for 2 hours at RT with gentle shaking to obtain HA-Gem-BSANPs (Scheme 1). The dispersion was lyophilized for 24 hours. The obtained formulations were stored at 2-8°C until further use.

**Experimental Design by Design Expert Software**

Central composite designs were employed to assess optimization parameters of Gem-BSANPs by using Design expert software-13. The objective of this design is to achieve optimum formulation with minimum particle size and maximum encapsulation efficiency. In this design, effect of three independent variables which consisting of pH of BSA solution, volume of ethanol and volume of BSA solution were investigated on response to dependent variables, including, particle size, encapsulation efficiency and NPs yield. The dependent and independent variables were selected based on our preliminary experimental work.

**Physicochemical Characterization of the NPs**

**i. Particle Size and Morphology**

The particle size, PDI and zeta potential of prepared NPs were recorded by using Zetasizer (Nano ZS, Malvern, Worcestershire, UK). The reconstituted NPs were dispersed in distilled water at 1.20 ratios and the analysis performed at 25°C and a 90-degree angle. The analysis was carried out in triplicate. Further morphology of the NPs was analysed by transmission electron microscopy (TEM). Prepared NPs were suspended in distilled water (5 mg/mL) with gentle shaking. 10 µL samples were deposited on a copper grid and excess samples were wiped out by using tissue paper and the grid was air dried. The TEM images were taken by using transmission electron microscope (Talos L120, Thermo Fisher Scientific).

**ii. Drug Loading and Encapsulation Efficiency**

Accurately weighed amount of NPs were dispersed in trypsin solution (0.1 mg/mg of NPs prepared in PBS, pH 4.7). The dispersion was kept on overnight, stirring at 37°C. The mixture was centrifuged (18000 rpm, 30 min) and the supernatant was analysed using LCMS as our previous reported method [20]. The drug loading was calculated as amount of Gem per mg of NPs. The encapsulation efficiency (% EE) was calculated by formula;

%EE = [{(total amount of Gem) - (amount of Gem in supernatant)}/total amount of Gem] × 100.

**iii. Differential Scanning Calorimetry (DSC)**

For the DSC analysis, the weighed quantity of Gem, HA, P'mix (physical mixture of HA, Gem and BSA), Gem-BSANPs and HA-Gem-BSANPs were kept into standard aluminium pans and heated from 40 °C to 350 °C (heating rate of 10 °C/min) with nitrogen as effluent gas (50 mL/min). The DSC (Mettler, Star1 SW 10.00) thermograms were recorded by a thermal system for a complete cycle.

***In vitro* Drug Release Profile**

For the in vitro release study, a specified amount of HA-Gem-BSANPs were suspended in 2 mL PBS, pH 7.4 to simulate physiological conditions and kept in a dialysis bag (MWCO 2 kDa). Similarly, to simulate tumor microenvironment pH, the specific amount of NPs was dispersed in 2 mL of PBS, pH 5.5 and kept in a dialysis bag (MWCO 2 kDa). The dialysis bag containing NPs dispersion was kept in the 100 mL PBS solution in a beaker at each pH condition. The bag then allowed for shaking (100 rpm) at 37 °C till the specified time period. To analyse the released drug into the media, 1 mL samples were taken out from the release media and replaced with the same media maintained at 37 °C. The sampling time points were 0.5, 1, 2, 4, 12, 24, 48, 72 and 96 hours. At each time point, the collected samples from the release media were analysed using the UPLC-MS/MS system (Waters, XEVO-TQD, MA, USA) as reported in our previous work [20].

***In vitro* Hemolysis Studies**

The hemolysis analysis of free Gem, Gem-BSANPs and HA-Gem-BSANPs were carried out as reported previously with few modifications [19]. Red blood cells (RBCs) were collected from mice into a micro vacutainer tube. The whole blood was centrifuged at 4000 rpm for 6 min at RT. The collected RBCs were repeatedly washed with PBS and prepared final dilution at the ratio of 1:10 in PBS, pH 7.4 The RBCs (1 mL solution) were then incubated with Gem, Gem-BSANPs and HA-Gem-BSANPs, each separately at a Gem equivalent concentration of 50µg/mL. The incubation was carried out for 2 hours at 37 °C in a shaker incubator. After completion of incubation, the samples were centrifuged at 4000 rpm for 6 min at RT. After centrifugation, 200 µL supernatant was withdrawn from each sample and analysed using a microplate reader at 576 nm. The percentage hemolysis was calculated by using the formula:

% Hemolysis = $100(A-A_0)/(A_{100}-A_0)$.

Where, $A_{100}$ and $A_0$ represent 100% and 0% hemolysis, respectively. A is absorbance of the treated samples.

***In vitro* Cytotoxicity Studies**

Cellular cytotoxicity of Gem, Gem-BSANPs and HA-Gem-BSANPs were carried out by MTT assay in A549 and MCF-7 cells as reported previously [19]. The cells were collected by trypsinization in DMEM media and 5000 cell per well were seeded into 96 well plates. For cells were kept for overnight incubation for 37°C in a $CO_2$ incubator for attachment of cells on surface of the well plates. On the second day, the media was withdrawn from the wells and the cells were incubated with different concentrations (0.01-100 µM) of Gem, Gem-BSANPs and HA-Gem-BSANPs for 48 hours. After treatment, the media were removed and MTT dye (120 µL, 0.5 mg/mL MTT solution in DMEM media) added and allowed the cells to have 2 hours of $CO_2$ incubation at 37 °C. The dye was withdrawn and DMSO solution (200 µL) added into each wells to lyse the cells. The intensity of colour was analysed using a TECAN microplate reader (Infinite M200 Pro) at 570 nm. The untreated

cells were considered as 100% viability (positive control) and % cell viability (CV) calculated by the formula: % CV = (Abs of treated cells at 570 nm /Abs of untreated cells 570 nm) × 100, mean ± SD, n=5.

**Nucleoside Transporter Inhibition Study**

Nucleoside transporter inhibition study has been assessed with MTT assay as per our previous report.[20] The A549 and MCF-7 cells were collected in DMEM media by trypsinization and 5000 cell per well were seeded overnight at 37°C in a $CO_2$ incubator on 96 well plates for surface attachment of the cells. On the second day, the cells were incubated with 10 μM dipyridamole for the first 30 min and then subsequently co-incubated with different concentrations of (0.01-100 μM) Gem, Gem-BSANPs and HA-Gem-BSANPs for 48 hours in a $CO_2$ incubator at 37 °C. After treatment the media was withdrawn from wells and 120 μL of MTT day (0.5 mg/mL MTT solution in DMEM media) were added. Finally, the cell cytotoxicity was analysed with MTT assay as stated earlier in the *in vitro* cytotoxicity studies section.

**Evaluation of Cell Apoptosis Activity**

The effect of Gem, Gem-BSANPs and HA-Gem-BSANPs on nuclear morphology of A549 and MCF-7 cells were observed using fluorescence dye 4′,6-diamidino-2-phenylindole (DAPI) as per previous report with slight modification [22]. Briefly, A549 and MCF-7 cells were incubated on 12 well plates and allowed for cell attachment by keeping into $CO_2$ incubator for overnight. Next day, the supernatant was withdrawn and the cells were incubated with Gem, Gem-BSANPs and HA-Gem-BSANPs (1 mM each Gem equivalent concentration). After 48 h of incubation, the cells were washed two times with PBS, pH 7.4, to remove unreacted formulations and drugs. The cells were fixed with 4% paraformaldehyde in PBS (pH 7.4) at 4 °C for 10 min. Finally, the cells were stained with DAPI and kept for 30 min in the dark and mounted on clean slides. Images have been captured with a fluorescence microscope (Nikon Eclipse Ti\\S) to observe change in nuclear morphology of the cells after treatment.

**Mitochondrial Membrane Potential (MMP) Loss Activities**

An MMP loss assay was performed to analyse changes in mitochondrial membrane of A549 cells after treatment of free Gem, Gem-BSANPs or HA-Gem-BSANPs. In a typical process, 2 x $10^5$ cells were seeded in 12 well plates. After surface attachment, the media were removed and the cells were treated with Gem, Gem-BSANPs or HA-Gem-BSANPs (1 μL each Gem equivalent) for 48 hours at 37°C in a CO2 incubator. After 48 hours of treatment, cells were collected and labelled with Rhodamine-123 dye. The fluorescence intensity was measured by using BD Biosciences, FACS, and loss in mitochondrial membrane potential was recored in terms of decrease of intensity.

**Statistical Analysis**

All the experiments were performed in triplicates and the data expressed as mean ± standard deviation (SD) in respective experiments. The statistical data were carried out using a one-way ANOVA test and the data were considered statistically significant when the P value was $< 0.05$.

## RESULTS AND DISCUSSION

### Preparation and Optimization NPs

Gem-BSANPs were processed with a desolvation cross-linking technique and glutaraldehyde is used for cross-linking agent for amino groups of the BSA. As reported earlier that the pH of BSA solution and quantity of ethanol added for desolvation of BSA has great effect on the formation of NPs [23]. The process variables were optimized in which the pH of the BSA solution varies from 6 to 10 and the result has been tabulated in Table 1. At acidic pH (pH 6), desolvation BSA was very difficult and there was no BSA precipitation observed even after the addition of 4 times more ethanol. At pH 6 (2 mL of BSA aqueous solution), the NPs formation is observed after the addition of 10 mL of ethanol. Similar observation was observed at pH 7, where 8 mL of ethanol is required for precipitation of 2 mL of BSA aqueous solution on continuous magnetic stirring. Further, less percent encapsulation efficiency observed at lower pH, which is 67.2±5.8 and 76.7±9.2 for pH 6 and 7, respectively. At the same time, large particle size was observed at lower pH, which was 214.6±6.4 and 184.3±7.2 at pH 6 and 7, respectively. At basic pH (pH 8, 9 and 10), less ethanol is required for precipitation of BSA, indicating that basic pH is required for the formation of NPs. The highest percent encapsulation efficiency (93.8±7.2) was observed at pH 9. Therefore, pH value 9, has been considered for preparation of optimized Gem-BSANPs. The cross-linking agent was 25% glutaraldehyde solution (100 µL) kept constant across the formulation process. After formation of NPs, the ethanol is evaporated by rotavapor, the dispersion was centrifuged and the obtained pellet was washed with PBS, pH 7.4 to remove unreacted glutaraldehyde and un-encapsulated drug. For coating of HA, the Gem-BSANPs pellets were dispersed in PBS pH 7.4 with HA (2 mg/mL) and the dispersion was incubated for 2 hours at 37°C with gentle shaking. The dispersion was finally freeze dried without adding any cryoprotectant and the coating has been confirmed by TEM analysis.

Design expert software-13 was used for the statistical design of experiments and data analysis in which Central Composite Design (CCD) was used to produce mathematical models that can be used to describe the relationship between the responses particle size, encapsulation efficiency and NPs yield. In order to design an optimum formulation and to predict the effect of independent variables which are pH of BSA solution, volume of ethanol and volume of BSA solution on dependent variables, including, particle size, encapsulation efficiency and NPs yield. Five different experiments were carried out in the lab by taking different pH (pH 6, 7, 8, 9 and 10) of BSA solution and determined the particle size, encapsulation efficiency and % yield of the NPs. Adequate precision, a measure of signal: noise ratio was greater than 4, which suggested that the model can be used to navigate the design space. All the responses had adequate precision values greater than 4, which indicated that the efficiency and suitability of the present model to obtain the desired attributes. 3D surface plot demonstrated that the formulation which was prepared at pH 9 showed the best result in terms of particle size (120.9±5 nm), encapsulation efficiency (93.8±7.2%) and % yield of the NPs (91.3±2.7%) and there was no significant difference observed between the experimental and predicted result (Fig. 1).

**Table 1**. Effect of process variables on preparation of NPs.

| **Parameters** | **Process variables and observation** | | | | |
|---|---|---|---|---|---|
| pH of BSA solution | 6.0 | 7.0 | 8.0 | 9.0 | 10.0 |
| Ethanol/BSA solution (v/v) | 2:10 | 2:8 | 2:6 | 2:5 | 2:5 |
| Particle size (nm) | 214.6±6.4 | 184.3±7.2 | 176.4±5.3 | 120.9±5.8 | 117.3±3.5 |
| (% EE) | 67.2±5.8 | 76.7±9.2 | 89.2±4.6 | 93.8±7.2 | 90.2±3.5 |
| NPs yield (%) | 78.6±3.5 | 82.6±7.7 | 88.3±5.6 | 91.3±2.7 | 89.7±8.2 |

**Table 2.** Fit model summary for analysis of response by design expert software-13

| **Responses** | **Sources** | **Sequential P- value** | **Adjusted $R^2$** | **Predicted $R^2$** | **Adequate precision** | **Result** |
|---|---|---|---|---|---|---|
| Particle size (nm) | Quadratic | 0.0009 | 0.8930 | 0.7967 | 9.5981 | Suggested |
| % EE | Quadratic | < 0.0001 | 0.9358 | 0.8780 | 11.090 | Suggested |
| NPs yield (%) | Quadratic | < 0.0001 | 0.9544 | 0.9133 | 16.449 | Suggested |

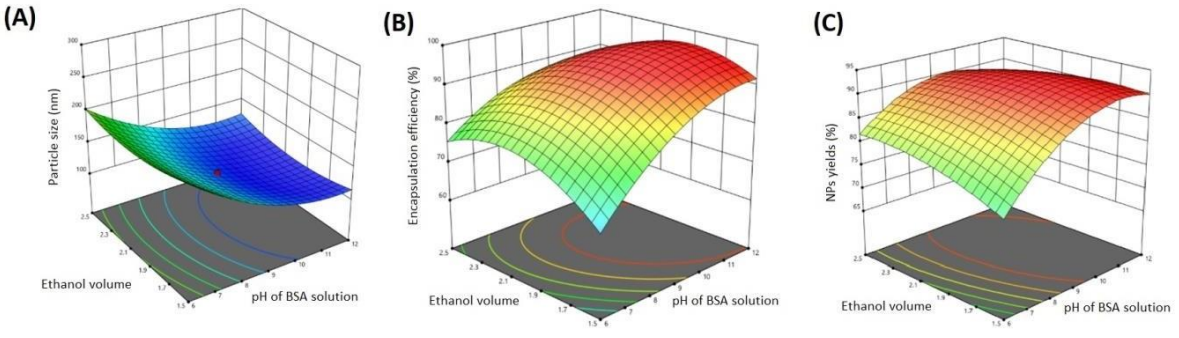


**Fig. 1** Response surface plots by using design expert software-13, showing the effect of different independent factors on **(A)** particle size (nm); **(B)** Encapsulation efficiency (%) and **(C)** Yield of NPs (%).

**Characterization of the NPs**

The prepared NPs were characterized by particle size, PDI, zeta potential while morphology was analysed with TEM analysis. The particle size and PDI of Gem-BSANPs gradually decreased while increasing the pH of the BSA solution during preparation of the NPs, which indicates a basic pH required for the formation of NPs (Fig. 2A.). The average particle size of optimized blank NPs and Gem-BSANPs were 118.3±6.35 nm and 120.9±5.87 nm, respectively. There was a slightly enlarged particle size (144.7±5.67 nm) that was observed after coating of HA on the surface of Gem-BSANPs (Table 3). The representative particle size of optimized HA-Gem-BSANPs has been depicted in Fig. 2B. The increased particle size of HA-Gem-BSANPs is due to bulkiness provided by HA, which indicates coating of HA on the surface of Gem-BSANPs. The Gem-BSANPs showed negative zeta potential, which becomes more negative after coating of HA (-28.66±1.10 mV and -45.72±3.24 mV for Gem-BSANPs and HA-Gem-BSANPs, respectively). The encapsulation efficiency of Gem-BSANPs was found to be 93.8±7.2% while 86.7±7.2% for HA-Gem-BSANPs. The drug

loading were 9.4% and 8.6% for Gem-BSANPs and HA-Gem-BSANPs, respectively. The decreased encapsulation efficiency of HA-Gem-BSANPs may be due to process loss during coating. The morphology of the NPs has been analysed by TEM analysis. The spherical shape of Gem-BSANPs was observed in TEM imaging (Fig. 2C). A HA layer was observed on TEM images of HA-Gem-BSANPs which confirmed the coating of HA on the surface of Gem-BSANPs (Fig. 2D).

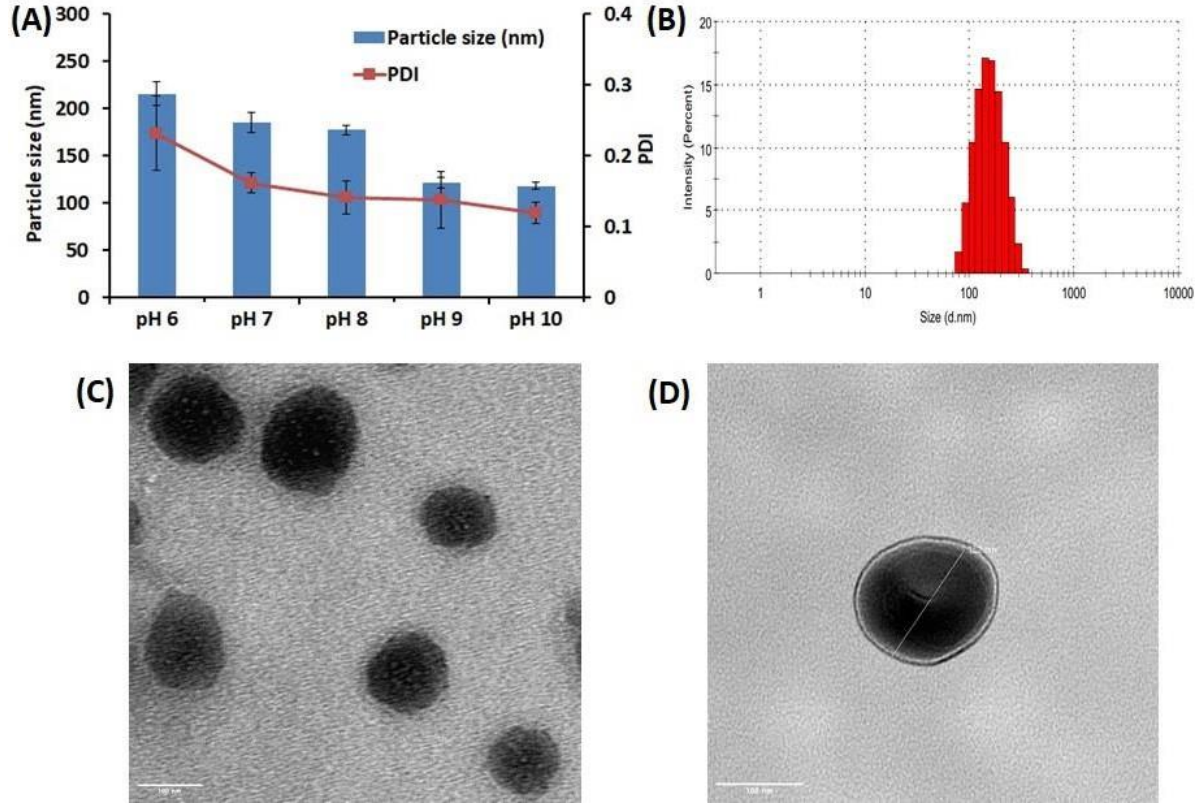


**Fig. 2 (A)** Effect of pH on droplet size reduction process on particle size and PDI of Gem-BSANPs; **(B)** A representative image of particle size of HA-Gem-BSANPs; (**C)** TEM image of optimized Gem-BSANPs; **(D)** TEM image of HA-Gem-BSANPs.

**Table 3.** Particle characterization of optimized NPs (n=3).

| **Formulation** | **Dilution factor** | **Particle size (nm)** | **PDI** | **Zeta Pot. (mV)** |
|---|---|---|---|---|
| Blank BSANPs | 1:20 | 118.3±6.35 | 0.094±0.02 | -29.42±0.62 |
| Gem-BSANPs | 1:20 | 120.9±5.87 | 0.137±0.04 | -28.66±1.10 |
| HA-Gem-BSANPs | 1:20 | 144.7±5.67 | 0.152±0.07 | -45.72±3.24 |

DSC analysis has been performed to determine the physical state of the Gem within the NPs. The Gem showed characteristics endotherm at 288 °C corresponding to its melting point indicated crystallinity of the Gem (Fig. 3). The scan of physical mixture also observed to have endothermic peak of Gem but these peaks were not observed in both NPs. Further shifting of HA peak observed after coating over the HA-Gem-BSANPs which confirms ionic and physical interaction of HA with Gem-BSANPs. The DSC data confirms an amorphous nature of Gem when encapsulated within the NPs. The amorphous form is beneficial for drug delivery application as it can be expected to have enhanced absorption and hence improved bioavailability of drugs [24].

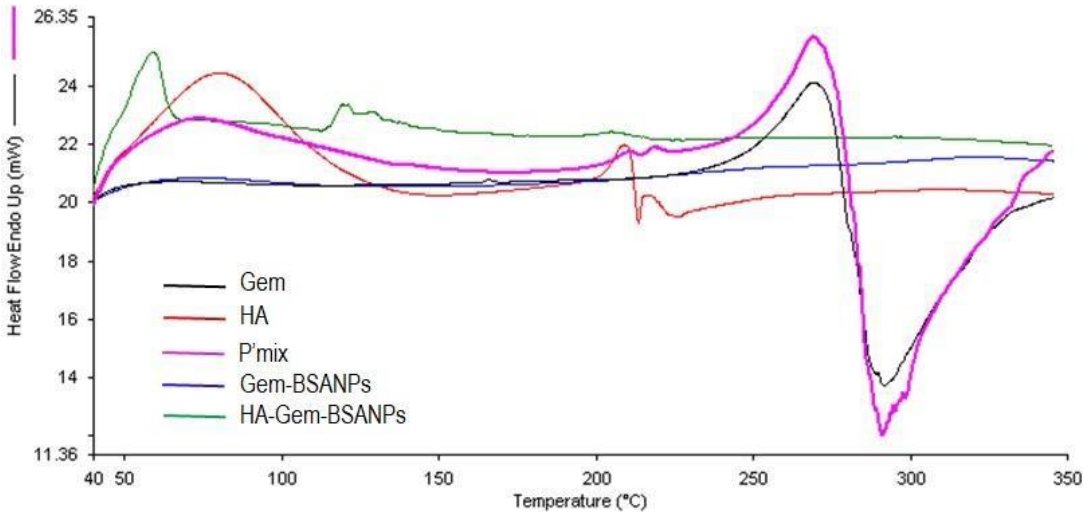


**Fig. 3.** DSC thermograms of Gem, HA, P'mix, Gem-BSANPs and HA-Gem-BSANPs. Accurately weighed samples were kept on a standard aluminium heating pan and heated from 40 °C to 350°C at the heating rate of 10 °C/min. The DSC thermograms were recorded using a thermal analysis system (Mettler, Star1 SW 10.00).

***In vitro* Drug Release Studies**

*In vitro* release of Gem from HA-Gem-BSANPs has been performed in PBS pH 7.4 and pH 5.5 to simulate physiological and tumor microenvironment pH conditions, respectively. The release profile demonstrated that Gem showed biphasic release from HA-Gem-BSANPs. The biphasic release pattern of Gem may be described as an initial fast release and then prolonged release. The release graph depicted that 25.3% and 32.7% of Gem had been released in the initial 4 hours from pH 7.4 and 5.5, respectively. The Gem showed controlled release in subsequent time point, *i.e.* 84.5% and 93.5% of Gem released from pH 7.4 and 5.5 respectively, after 96 hours (Fig. 4). The release of Gem at pH 5.5 is higher as compared to physiological pH. This could be due to breakage of polymeric bonds at lower pH. The initial burst release of Gem might be due to a loosely bounded and surface associated drug to the NPs while the drug present in a core of NPs showed prolonged release profile.

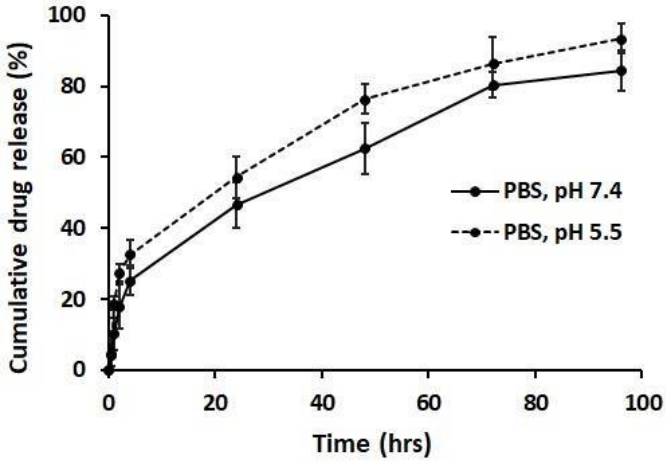


**Fig. 4** *In vitro* release profile of Gem from HA-Gem-BSANPs in PBS, pH 7.4 and 5.5. The samples from the release media were taken out at a specified time point and quantification of Gem has been done by using UPLC-MS/MS.

***In vitro* Hemolysis Studies**

Gem in the circulatory system shows dose-limiting haematological toxicity [25]. The Gem-BSANPs and HA-Gem-BSANPs demonstrated significantly low hemolysis as compared to free drugs. The low hemolysis is due to encapsulation of the Gem in the NPs and hence fewer drugs are available for interaction with RBCs. The result showed that Gem has 18.4 percent hemolysis as compared to 7.2 and 6.8 percent of Gem-BSANPs and HA-Gem-BSANPs, respectively, at concentration of 50 µg/mL (Fig. 5). Blank BSA NPs exhibited less than 2% hemolysis. Hemocompatibility of Gem is improved by encapsulation into BSA NPs, which could be beneficial in intravenous administration of the NPs [26].

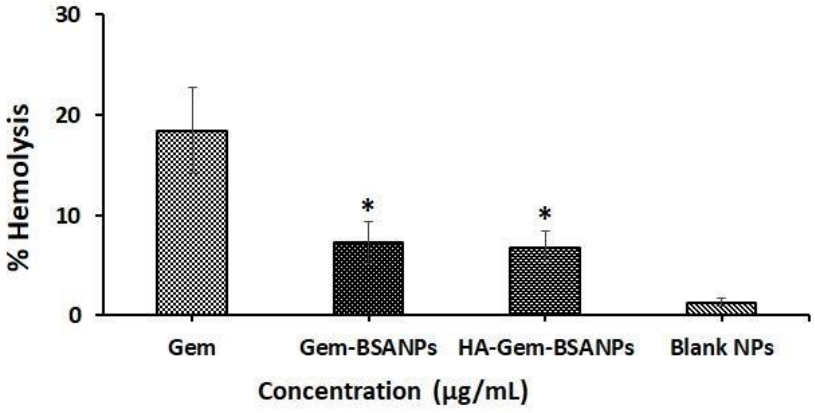


**Fig. 5** Hemolysis activities of Gem, Gem-BSANPs and HA-Gem-BSANPs on RBCs. The RBCs were collected from fresh blood of mice and incubated with free Gem, Gem-BSANPs and HA-Gem-BSANPs at 37 °C for 2 hours.

***In vitro* Cytotoxicity Studies**

Cell cytotoxicity activity of Gem-BSANPs and HA-Gem-BSANPs were carried out in A549 and MCF-7 cells by MTT assay. The cells were treated for 48 hours and it was observed that the NPs exhibited more cytotoxicity than the free Gem (Fig. 6). The higher cytotoxicity of the Gem-BSANPs and HA-Gem-BSANPs is due to improved cellular internalization and accumulation of the NPs in cells. Similar results were also observed where the cytotoxicity of the Gem has been improved by using NPs due to enhanced cell uptake and retention inside the cells [27,28]. The hampered cytotoxicity of free Gem may be due to less cellular internalization and into the cells [29]. In particular, higher toxicity of HA-Gem-BSANPs were observed in A549 cells as compared to MCF-7 cells this may be because of A549 cells have higher level of CD44 expression as compared to MCF-7 cells [30]. The cytotoxicity result demonstrated that the encapsulation of Gem inside into the BSA and coating with HA could be a potential strategy for improved cancer chemotherapy by Gem.

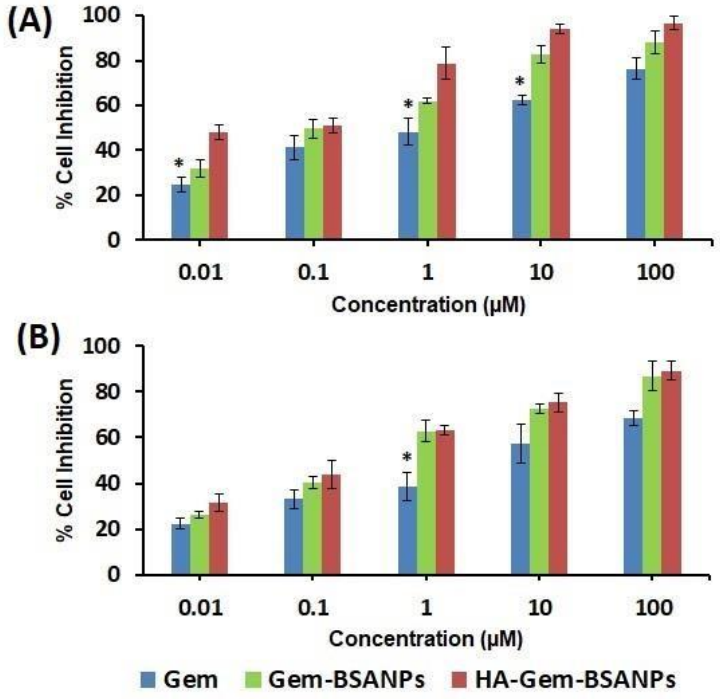


**Fig. 6** *In vitro* cytotoxicity studies on **(A)** A549 and **(B)** MCF-7 cells. The cells were treated for 48 hours and MTT assays were performed to assess cytotoxicity of the treatment at different concentrations (0.01, 0.1, 1, 10, 100 μM). The graph depicted % cell inhibition *vs* concentration (μM).

**Nucleoside Transporter Inhibition Study**

Entry of Gem in cells is an energy dependent process and hence a nucleoside is needed for the uptake of free Gem into the cells. To demonstrate the mechanism of how Gem or its NPs enter into the cells, a nucleoside transporter inhibition study was performed. For this study, dipyridamole was used to block the nucleoside transporter site which is a non-specific nucleoside transporter inhibitor (hENT1) [31]. For the study, the cells were first pre-incubated with dipyridamole followed by co-treatment by Gem, Gem-BSANPs or HA-Gem-BSANPs at different concentrations of (0.01-100 μM). The cytotoxic activity of Gem was retarded due to non-availability of nucleoside. At the same time, the actions of Gem-BSANPs and HA-Gem-BSANPs were not affected. The dependency of Gem on nucleoside transporters was hampered or the lack of the presence of nucleoside is the main reason for drug resistance [8]. The result showed that HA-Gem-BSANPs have lower cell viability as compared to both Gem as well as Gem-BSANPs in A549 and MCF-7 cell lines (Fig. 7). The study advocated that the Gem required a nucleoside to be internalized into the cell, while the NPs do not depend on transporters for cellular internalization.

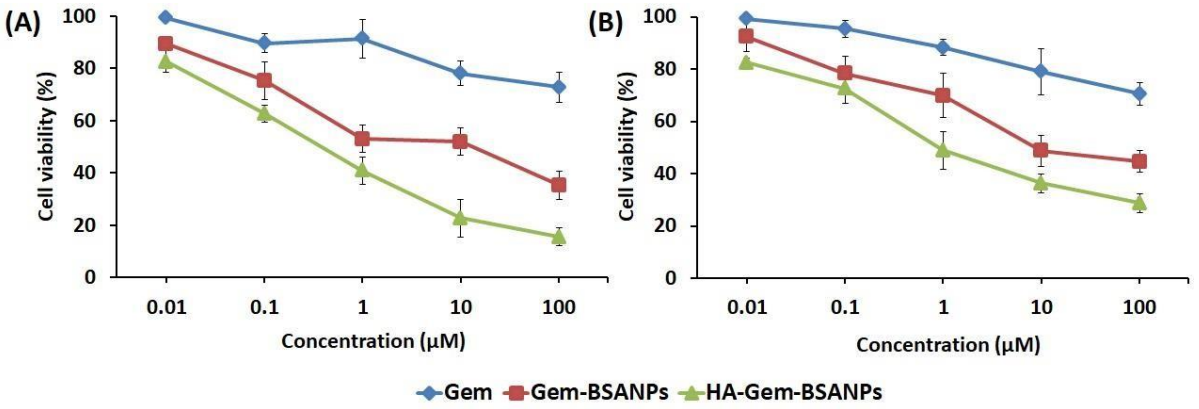


**Fig. 7** Nucleoside transporter inhibition studies on (A) A549 and (C) MCF-7 cells. Dipyridamole was taken as a nucleoside transporter inhibitor and the cells were pre-treated, followed by co-treated with different concentrations of Gem, Gem-BSANPs and HA-Gem-BSANPs for 48 hours. Cell viability (%) was measured by MTT assay and the dats was written as mean±SD (n = 5).

**Evaluation of cell apoptosis**

Apoptosis is a key mechanism for chemotherapy induced cell death. In the process of apoptosis, several biochemical events occur leading to changes in cell morphology and death. The A549 and MCF-7 cells were used to determine whether NPs promote the induction of apoptosis. The cells were treated for 48 h at the concentration of 1 μM of free Gem, Gem-BSA-NPs and HA-Gem-BSANPs. For the analysis, apoptotic A549 and MCF-7 cells were stained DAPI after treatment. The images were acquired by using a fluorescence microscope (Nikon Eclipse Ti-S). The result demonstrated that HA-Gem-BSANPs treated cells induced higher apoptosis compared to free Gem (Fig. 8) in both cell lines. Moreover, the A549 cells treated with HA-Gem-BSANPs show more apoptotic nucleus as compared to MCF-7 cells. The higher apoptosis may be due to the fact that A549 cells overexpress CD44 receptor on their surface and hence facilitate receptor mediated endocytosis of HA-Gem-BSANPs.

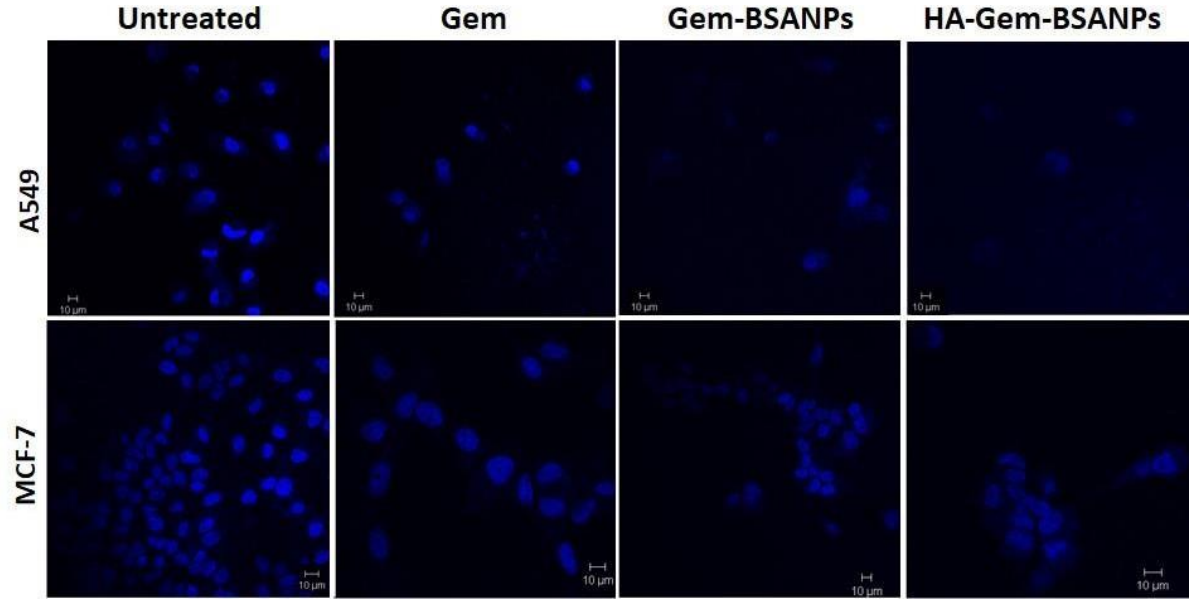


**Fig. 8** Effect of Gem, Gem-BSANPs and HA-Gem-BSANPs on the nuclear morphology of A549 and MCF-7 cells after 48 hours. For the analysis, apoptotic A549 and MCF-7 cells

were stained DAPI after treatment. The images were captured by using fluorescence microscope (Nikon Eclipse Ti-S). Scale bar: 10 μm.

**Mitochondrial Membrane Potential Loss Activity**

The mitochondrial potential loss is indicative of apoptosis in cells. The MMP is an indicator of cell health and hence, we tested the effect of free Gem, Gem-BSANPs and HA-Gem-BSANPs on mitochondrial membrane. The treatment with a cytotoxic drug cause opening of pores of the mitochondrial membrane, leading to leakage of mitochondrial material into the cytosol, resulting in the initiation of cell death [32]. Since A549 overexpresses the CD44 receptor on its surface, hence only this cell line is used for the MMP loss assay. The Rhodamine dye was used to perform MMP loss assay because it can internalise into mitochondria and intensity is directly proportional to the MMP loss. The result showed that HA-Gem-BSANPs are able to induce higher mitochondrial potential loss as compared to Gem-BSANPs and free Gem (Fig. 9) and hence are able to produce apoptosis in cancer cells.

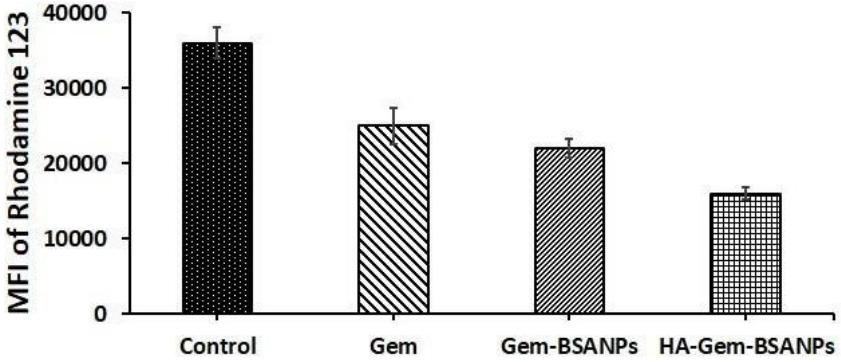


**Fig. 9** The effect of free Gem, Gem-BSANPs and HA-Gem-BSANPs on mitochondrial membrane potential loss in A549 cells. The cells were treated with 1 μL concentration each of Gem, Gem-BSANPs or HA-Gem-BSANPs for 48 hours at 37°C and then labelled with Rhodamine 123 dye.

**Objective 2:** Preparation, characterization and evaluation of Gem conjugated self-assembled nanoparticles for anticancer activity.

**Method**

***In vivo* Anti-tumor Activity**

The in vivo therapeutic efficacy Gem conjugated self-assembled NPs was performed in 4T1 tumor-bearing Balb/c mice model. The animals were given standard food and water and monitored before starting the study. The 4T1 cells were cultured in DMEM medium, and 1× 106 cells in 0.1 mL normal saline, were transplanted in the right thigh of mice intramuscularly. The animals were then randomly divided into groups (n = 6): (i) untreated (saline); (ii) Blank NPs (treated with equivalent amount of blank NPs); (iii) free Gem (treated with 5 mg/kg); (iv) Gem conjugated self-assembled NPs (treated with equivalent to 5 mg/kg of free Gem). Each group was given the respective treatment via the intraperitoneal route for four doses on days 0, 3, 7 and 10. Mice body weight was analysed on days 0, 3, 6, 9 and 14 while tumor volume was recorded on day 3, 6, 9 and 14. On the 14th day, after body weight measurement, the tumor-bearing thighs of the mice were measured as the longest (a) and

shortest diameters (b) of the tumor by using vernier callipers. The size of tumor was represented as tumor volume (V = 1/2[a × b2]). At the end of the study, the mice were sacrificed and major organs, including the heart, liver, kidney and spleen were isolated and processed for histopathology.

**Histological Examination of Major Organs**

To observe the clinical efficacy and safety of Gem conjugated NPs, histopathological examination of the mice was performed after treatment. At the experimental endpoint, we sacrificed the mice and the major organs, including, the heart, kidney, liver, and spleen were excised. The excised organs (5 mm size of 2 pieces) were rinsed thrice with PBS (pH 7.4) and then fixed with neutral formalin buffer (10%). The sections of excised tissues were carried out for haematoxylin & eosin (H&E) staining. The images of stained sections of the organs were analysed using a Microscope (Leica Microscope Microsystems, UK).

## RESULT AND DISCUSSION

### *In vivo* Anti-tumor Activity

The therapy study of Gem and Gem conjugated self-assembled NPs was performed in 4T1 tumor-bearing Balb/c mice. After tumor implantation, the animals has been then randomly divided into four groups: (i) untreated (saline); (ii) free Gem (treated with 5 mg/kg); (iii) blank nanoparticles (treated with an equivalent amount of blank NPs); (iv) Gem conjugated self-assembled NPs (treated with equivalent to 5 mg/kg of free Gem), and total 4 doses of treatment given. The schematic representation for the experimental design has been demonstrated in Figure 9A. The mice treated with Gem conjugated self-assembled NPs exhibited the lowest size of tumor (Figure 9B). The untreated (saline) and blank NPs treated mice have fast tumor growth with an average tumor volume of 1098.2±334.7 mm3 and 1056.2± 151.3 mm3, respectively, on day 14. However, the mice treated with Gem showed an average tumor volume of 718.1± 168.5 mm3 while Gem NPs exhibited 458.6±103.2 mm3 (Figure 9C). These results demonstrated significantly delayed tumor growth for the mice treated with multiple injections of Gem NPs as compared to a free drug at the same dose. Similarly, approximately 1.7-fold higher tumor growth inhibition was observed with nano-particulate formulations, which are 58.2% and 34.6% for Gem NPs and free Gem, respectively (Figure 9D). Tumor volume gradually increased and there was no significant difference in tumor volume between saline and blank NPs treated groups. The mice treated with Gem NPs showed significantly lower tumor volume as compared to native Gem (Figure 9E). The enhanced anticancer potential of the Gem conjugated self-assembled NPs is because of the protection of drugs from cytidine deaminase in the circulatory system and hence followed by the targeted drug delivery to the tumor cells. The survival of mice and change in the mice's body weight across the group of live animals has been also observed during the therapy experiment (Figure S6 and S7). There was no significant change observed in mice's body weight following any of these treatments while the survival of mice treated with Gem or Gem NPs, 4 times more than untreated mice.

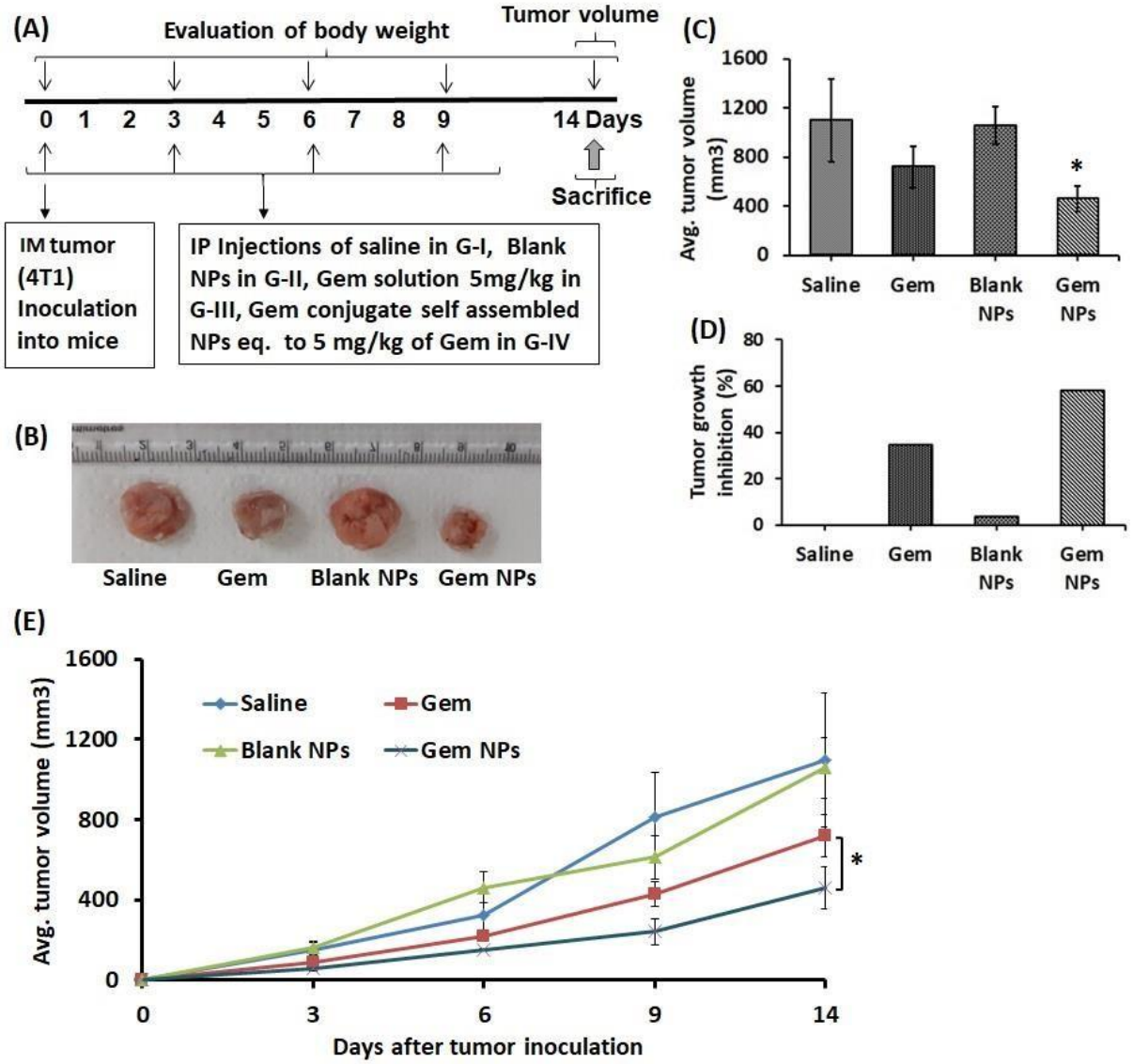


Figure 10. Evaluation of in vivo efficacy of Gem and Gem conjugated self-assembled in 4T1 tumor-bearing Balb/c mice. (A) Schematic representation for the experimental design of the study; (B) Representative photograph of excised 4T1 tumor after therapy at day 14; (C) Average tumor volume after therapy on day 14; (D) Graph of percentage tumor growth inhibition; (E) Tumor growth curve after 4T1 tumor inoculation.4T1 cancer cells were intramuscularly inoculated into Balb/c mice at day 0. Total four doses to Group-1 saline, Group-II Gem solution, Group-III blank NPs and Group-IV Gem conjugated self-assembled NPs. Data are represented as mean value ±SD (n=6). The statistics are one-way ANOVA, (*) $p < 0.05$ Gem versus Gem conjugated self-assembled NPs.

**Histological Examination of Major Organs**

Histopathology examination of heart, kidney, liver and spleen of 4T1 tumor-bearing Balb/c mice were examined after the therapeutic efficacy of the Gem and Gem conjugated self-assembled NPs. As depicted in Figure 10, there are no histological abnormalities were observed in major organs after treatment across the groups. These results confirm the biocompatibility and non-toxic nature of the NPs.

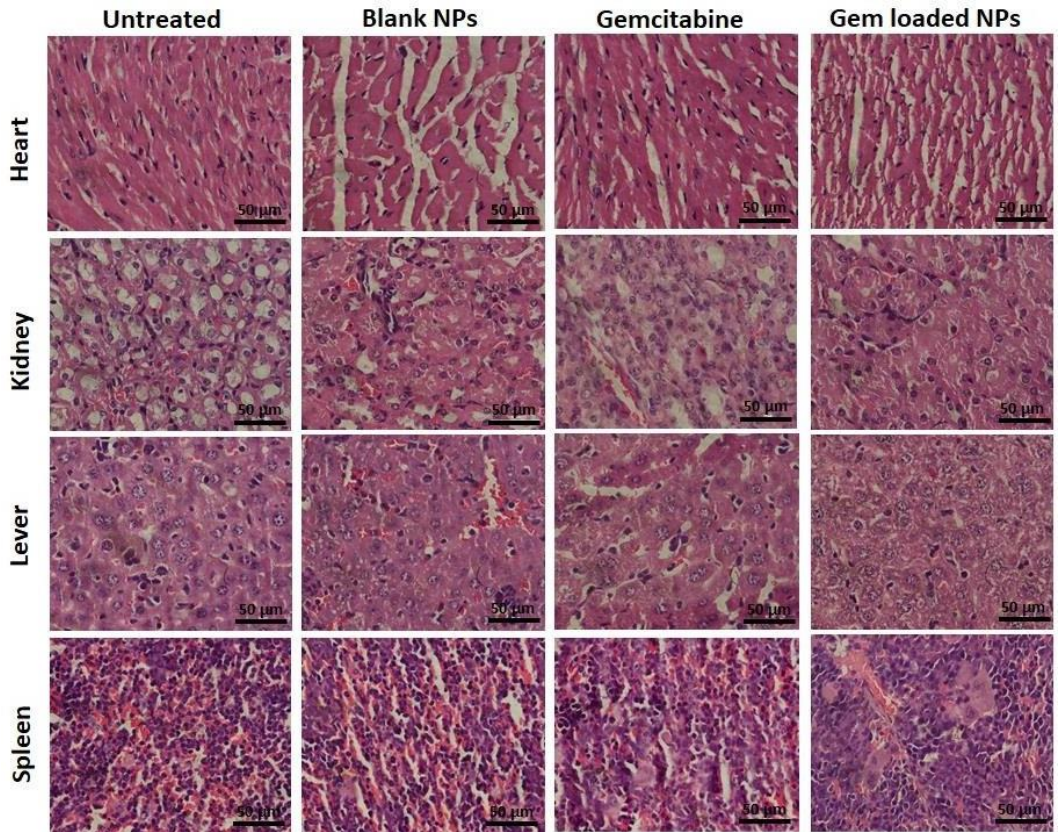


Figure 11: Histopathology examination of the heart, kidney, liver and spleen of 4T1 tumor-bearing Balb/c mice were examined after the therapeutic efficacy study. Mice were treated with saline, blank NPs, Gem and Gem conjugated self-assembled NPs for a total of 4 doses. At the experimental endpoint, the major organs were excised from the individual group, and the tissue sections were stained with haematoxylin and eosin (H & E). The images of stained sections were observed under a Leica DM Microscope (Leica Microsystems, UK). Scale bar: 50 µm.

## 5. Conclusion:

**Objective-I**

- Hyaluronic Acid coated bovine serum albumin Nanoparticles has been prepared characterized and evaluated for anticancer activity.
- The HA-Gem-BSANPs found to be more effective then Gem-BSANPs and Gem alone on anticancer activity.

**Objective-II**

- Gemcitabine conjugated self-assembled nanoparticles has been prepared, characterized and evaluated for their anticancer activity
- The nanoparticulate formulation found to be more effective then free Gem in anticancer activity.

## References


1. Liu CG, Han YH, Kankala RK, Wang S bin, Chen AZ. Subcellular Performance of Nanoparticles in Cancer Therapy. Int J Nanomedicine; 2020; 15:675–704. Available from: https://doi.org/10.2147/ijn.s226186
2. Carmichael J, Fink U, Russell RCG, Spittle MF, Harris AL, Spiessl G, et al. Phase II study of gemcitabine in patients with advanced pancreatic cancer. Br J Cancer; 1996; 73:101–5. https://doi.org/10.1038/bjc.1996.18
3. Yardley DA. Gemcitabine Plus Paclitaxel in Breast Cancer. Semin Oncol.; 2005;32:14–21. https://doi.org/10.1053/j.seminoncol.2005.06.025
4. Ozols RF. Gemcitabine and carboplatin in second-line ovarian cancer. Semin Oncol; 2005; 32:4. Available from: https://doi.org/10.1053/j.seminoncol.2005.06.023
5. Hoang T, Kim KM, Jaslowski A, Koch P, Beatty P, McGovern J, et al. Phase II study of second-line gemcitabine in sensitive or refractory small cell lung cancer. Lung Cancer; 2003; 42:97–102. https://doi.org/10.1016/s0169-5002(03)00273-3
6. Heinemann V, Xu YZ, Chubb S, Sen A, Hertel LW, Grindey GB, Plunkett W. Cellular Elimination of 2',2'-Difluorodeoxycytidine 5'-Triphosphate: A Mechanism of Self-Potentiation. Cancer Research 1992; 52: 533–9.
7. Neff T, Blau CA. Forced expression of cytidine deaminase confers resistance to cytosine arabinoside and gemcitabine. Exp Hematol. 1996; 24:1340–6.
8. Mackey JR, Mani RS, Selner M, Mowles D, Young JD, Belt JA, Crawford CR, Cass CE Functional Nucleoside Transporters Are Required for Gemcitabine Influx and Manifestation of Toxicity in Cancer Cell Lines. Cancer Research. 1998; 58: 4349–4357.
9. Bregadze VI, Sivaev IB, Dubey RD, Semioshkin A, Shmal'ko A v., Kosenko ID, et al. Boron-Containing Lipids and Liposomes: New Conjugates of Cholesterol with Polyhedral Boron Hydrides. Chemistry – A European Journal; 2020; 26:13832–41. https://doi.org/10.1002/chem.201905083
10. Dubey RD, Sarkar A, Shen Z, Bregadze VI, Sivaev IB, Druzina AA, et al. Effects of Linkers on the Development of Liposomal Formulation of Cholesterol Conjugated Cobalt Bis(dicarbollides). J Pharm Sci.; 2021; 110:1365–73. https://doi.org/10.1016/j.xphs.2020.12.017
11. Dubey RD, Saneja A, Qayum A, Singh A, Mahajan G, Chashoo G, et al. PLGA nanoparticles augmented the anticancer potential of pentacyclic triterpenediol in vivo in mice. RSC Adv.; 2016; 6:74586–97. https://doi.org/10.1039/C6RA14929D
12. Nahire R, Haldar MK, Paul S, Ambre AH, Meghnani V, Layek B, et al. Multifunctional polymersomes for cytosolic delivery of gemcitabine and doxorubicin to cancer cells. Biomaterials; 2014; 35:6482–97. https://doi.org/10.1016/j.biomaterials.2014.04.026
13. Wang Y, Fan W, Dai X, Katragadda U, McKinley D, Teng Q, et al. Enhanced tumor delivery of gemcitabine via PEG-DSPE/TPGS mixed micelles. Mol Pharm; 2014; 11:1140–50. https://doi.org/10.1021/mp4005904
14. Jia L, Zheng JJ, Jiang SM, Huang KH. Preparation, physicochemical characterization and cytotoxicity in vitro of gemcitabine-loaded PEG-PDLLA nanovesicles. World J Gastroenterol; 2010; 16:1008–13. https://doi.org/10.3748/wjg.v16.i8.1008
15. Dubey RD, Klippstein R, Wang JTW, Hodgins N, Mei KC, Sosabowski J, et al. Novel Hyaluronic Acid Conjugates for Dual Nuclear Imaging and Therapy in CD44-Expressing Tumors in Mice In Vivo. Nanotheranostics; 2017; 1:59–79. https://doi.org/10.7150/ntno.17896


6/12/2022

**Signature**
**Shweta Paroha**
**(Ph.D. Scholar)**

**Signature**
**Prof. P. K. Sahoo**
**(Supervisor)**

Scanned with OKEN Scanner